Journal of the Earth & Space Physics. Vol. 32, No. 3, 2006, P. 23-32

Crustal seismic anisotropy in the south-central Alborz region using Moho P_s converted phases

Sadidkhouy, A[*]., Javan Doloei, Gh[**]. and Gheitanchi, M. R[*].

[*]*Institute of Geophysics, University of Tehran, P.O. Box 14155- 6466, Tehran, Iran*
[**]*International Institute of Earthquake Engineering and Seismology (IIEES), Tehran, Iran*

(Received: 31 Jan 2006 , Accepted: 19 Sep 2006)

Abstract

In this paper to find stable anisotropy direction with minimum error, we attempt to automate the choice of analysis of Moho P_s phase window by performing a grid search over different windows. We have determined the anisotropy direction in the crust of the Alborz region by using 8 events recorded at three IIEES seismic broadband stations (i. e. DAMV, THKV and CHTH).

Analysis of shear wave splitting of the Ps conversion from the crust-mantle boundary indicates a fast azimuth of anisotropy oriented approximately NE-SW. This strongly suggests coherent crustal anisotropy with a fast direction perpendicular to the strike of mountain block ranges.

We estimate the average directions of anisotropy under three stations, DAMV, THKV and CHTH of 42, 55, 55 degree, respectively. Moreover our results show that the magnitude of anisotropy are 0.23, 0.22, 0.27 seconds, respectively, which are in good agreement with the geology and tectonic setting of this region.

Key words: Anisotropy, Shear wave splitting, P_s converted phase, Grid searching, Anisotropy direction and magnitude, Receiver function

1 INTRODUCTION

One of the best ways to study deformation in the Earth‘s interior is detection and interpretation of seismic anisotropy, or the dependence of seismic velocities on wave propagation and polarization direction. Deformation-induced fabric in the crust and mantle likely causes seismic anisotropy. The characterization of seismic anisotropy within the Earth provides essential clues to the Earth’s dynamic evolution. Over the past several decades, significant progress has been achieved in obtaining clearer images of seismic anisotropy, but in many cases, the location of anisotropic structures has been poorly resolved. Another significant issue is that the connections between anisotropy observations and deformational processes are still under debate. The structural origin of seismic anisotropy is therefore still not well known (Fouch and Rondenay, 2005).

This is a mounting body of evidence suggesting that seismic isotropy may actually be a rarity rather than the rule in the shallow earth. The majority of minerals and rocks forming the crust and upper mantle display seismic anisotropy in laboratory measurements (Babuska and Cara, 1991). Anisotropy in the oceanic crust and lithosphere was established by marine refraction experiments over two decades ago (e.g., Raitt et al., 1969). Shear-wave splitting in broad-band seismic data suggests that the continental lithosphere has significant elastic anisotropy (e.g., Vinnik et al., 1992; Silver, 1996), which can be used to reconstruct both active and fossil bulk strain. The upper part of the continental crust appears to have particularly strong anisotropic properties (Zhi and Schwartz, 1994; Lynn, 1991).

The variety of mechanisms producing seismic anisotropy in the crust centers depends on a handful of scenarios. In the upper crust the strongest influence is believed to be that of aligned cracks and/or pore spaces (Babuska and Pros, 1984), for which slower velocities are found for waves that propagate normal to average crack plane. The aspect ratio of pore, cracks and presence of fluid in them determine the extent and proportion of anisotropy (Hudson, 1981; Crampin, 1984a, 1991). Alternating thin isotropic layers of higher and lower velocity can also produce an overall anisotropic effect (Backus, 1962), with the velocities slower normal to bedding than along it. In the lower crust and the uppermost mantle, cracks are assumed to close in response to increasing overburden pressure (Babuska and Pros, 1984), though field exposures

of (formerly) deep-crustal fluid-filled cracks can be found (Ague, 1995). In the absence of cracks and inclusions, the lattice-preferred orientation (LPO) of mineral crystals is taken as the main cause of seismic anisotropy. Most minerals composing the bulk of the crust are anisotropic to some degree (Babuska and Cara, 1991), while properties of olivine and, to a lesser extent, orthopyroxene dominate the upper mantle anisotropy. Different deformation mechanisms can lead to the alignment of either the slow or the fast crystallographic direction in olivine grains (Ribe, 1992), but LPO caused by dislocation creep in the shallow mantle is commonly believed to lead to preferred alignment of the fast axis (Zhang and Karato, 1995).

Our scientific objectives focused on using P to S conversions in the coda of the teleseismic P wave to better define the structure and active tectonic processes in the Alborz Region. Within this context, this paper examines shear wave splitting observed in P to S converted phases (Ps phases) generated at the crust-mantle boundary. These observations are unique in that the source of the shear wave splitting must lie above the Moho. Thus they provide an excellent means of studying the nature of vertically averaged shear wave anisotropy in the crust. A Ps phase propagating through anisotropic medium splits into a fast phase and a slow phase that becomes increasingly separated in time as the wave propagation. In this study we used the automated Ps-phase splitting technique to analysis the data.

We used the receiver function analysis, which becomes a common method of examining crust and upper mantle structure. This method is applied to a single three-component seismic station, and can estimate crustal thickness and occasionally other first-order details of the continental crust (Phinney, 1964; Burdick and Langston, 1977; Langston, 1977, 1979). With the advent of broadband digital seismic stations in the early 1980s, higher resolution crustal models could be determined beneath isolated stations (Owens et al., 1984; Owens, 1987).

Previous geological and geophysical studies beneath the Alborz give us a general view of the crustal and uppermost mantle structure across this area. Due to lack of knowledge from parameters of anisotropy in the Alborz region, study of this branch of seismology is very important. In this paper we have estimated the anisotropy parameters using Ps converted waves in the Alborz region.

2 TECTONICS SETTING OF ALBORZ REGION

The Alborz is a narrow mountain range only 100 km wide which wraps around the South Caspian Sea (figure 1). The mean elevation in the Alborz drops sharply from 3000 m in the inner belt to -28 m at the Caspian shoreline to the North. The topographic contrast is less pronounced to the south where the connection with the lowlands of the Central Iranian desert is progressive. The Alborz mountains are branche of the Alpine Himalayan orogeny in Iran. Iran lies within the continental collision zone between Africa and Eurasia. Active faulting, recent volcanism, and high surface elevations are important characteristics of this area. Geomorphic and trenching investigations along the Kahrizak fault, which is located south of Tehran, provided some new constraints on the activity of this region (De Martini et al., 1998). A general study of seismic P-wave and S-wave velocities by using arrival time data of regional earthquakes provided seismic structure information beneath Iran with average Pn velocity of 8.0 ± 0.1 km/s (Chen et al., 1980). Surface wave analysis of a few events suggested a one-layer model crust with 45 km thickness beneath the eastern part of Alborz mountain range. Asudeh (1982) showed that the crust and upper mantle in the eastern part of Iran are characterized by low body wave velocities. The gravity field and crustal structure of Iran, in the study by Dehghani and Makris (1984), showed that the Bouguer gravity along the Alborz mountain range varies between-100 and -120 mgal and the crustal thickness is less than 35 km beneath the northern Alborz. Surprisingly, no crustal root has been detected below the high topography, and the compensation mechanism remains conjectural. Recent tectonic history is thought to be separated into two phases: a Miocene North-South compression between the central Iranian Block and the South Caspian Basin; a Pliocene and Quaternary North-East shortening oblique to the E-W structures of the central Alborz (Jackson and McKenzie, 1984 and Allen et al., 2003).

Numerical modelling of the deformation of the Iranian plateau identified that crustal thickening and shear deformation tend to localize near the southwest of the country. Their results specified a 45-km crustal thickness along the Alborz mountain range (Sobouti and Arkani-Hamed, 1996). Based on receiver function analysis of teleseismic data, Mangino and Priestley (1998) provided more information on

the crustal structure of the southern Caspian region in the north of the Alborz mountain range. The results of receiver function inversion of teleseismic P-waves recorded in ILPA (Iranian Long Period Array) has shown 47 ± 2 km crustal thickness for southwest of the Tehran region (Doloei and Roberts, 2003). Furthermore, Sodoudi et al. (2004) obtained a detailed Moho depth map beneath this area using teleseismic receiver function. They estimated an average crustal thickness of 48 km under the central Alborz.

Knowledge of the strain pattern in Iran is rapidly improving due to repeated GPS measurements recently done in Iran and several key areas such as the central Zagros, the Zagros-Makran transition and the Alborz are under geodetic investigation. At the longitude of the Persian Gulf, Arabian and Eurasian plates collide at a rate of ≈ 22 mm/year, compatible with recent geodetic studies. This short-term rate is also in fairly good agreement with the long-term rates of 20-31 mm/year provided by plate reconstruction (DeMets et al., 1990 and McQuarrie et al., 2003).

A outstanding feature provided by these surveys is the quasi-rigid behavior of the Sanandaj-Sirjan zone in Central Iran that moves to the north with respect to Eurasia at a velocity of 14 ± 1 mm/year. As already proposed, the foregoing study demonstrates that no motion to the east can be detected for the Central Iranian Block suggesting that the Lut and Helmand blocks do not allow an eastward displacement of the Central Iranian Block. Therefore, the Helmand block acts like an eastward-locked boundary condition. This implies that the deformation of the Alborz and Kopet Dag mountains must be explained in the framework of the northward shortening between the Central Iranian Block and the Eurasian plate (Vernant et al., 2004).

The direction of horizontal projection of slip vectors in the Alborz region is shown in figure 2. These directions are calculated by different methods such as body wave modeling, Harvard CMT solution and first motion solution (Jackson et al., 2002).

3 SHEAR WAVE VELOCITY ANISOTROPY USING P_s PHASE

We present a method for automating the selection of the window to calculate shear wave velocity anisotropy. First, the splitting analysis is applied in order to find those measurements which are stable over many different windows. Once clusters of stable results have been found the final choice of shear wave analysis window corresponds to the measurement with the lowest error in the cluster with the lowest variance.

Analysis of shear wave splitting on local and teleseismic shear waves has evolved into a very commonly used tool for constraining continental seismic anisotropy (e.g., Silver and Chan, 1988; Vinnik et al., 1989; Savage et al., 1990; Vinnik et al., 1992; Levin et al., 1999; Fouch et al., 2000). Methods of shear wave splitting analysis can be divided into three main groups, where the search for the optimal pair of splitting parameters is based on: 1-the minimization of a penalty function which represents the difference between observed and predicted transverse components (e.g., Vinnik et al., 1989); 2-the maximization of the cross- correlation between the fast and slow components or linear particle motion (e.g., Bowman and Ando, 1987; Levinet al., 1999); and 3-the minimization of energy on the corrected transverse component reassembled from the optimal fast and slow components (e.g., Silver and Chan, 1988; Silver and Chan, 1991). We note that this last method can be applied to P-to-S (P_s) converted waves where transverse energy results primarily from seismic anisotropy.

Figure 3 schematically shows the effects of shear wave splitting on Moho P_s phases. Initially, a near-vertically incident P wave generates a radially polarized converted shear wave at the crust-mantle boundary. The shear wave upon entering the anisotropic region splits into two phases with polarizations and velocities that mimic the properties of the anisotropic media. The phases, polarized into fast and slow directions, progressively split in time as they propagate through the anisotropic media. This split is preserved in any isotropic segments along the ray path and can be observed as a time delay (δt) between the two horizontal components of motion (figure 3). Polarity and amplitude are strongly affected by the azimuth of arrival. Anisotropy also leaves a characteristic signature on the tangential component of receiver functions. In contrast to the case of a dipping layer, the tangential component will be zero along both the fast and slow azimuth directions and reach a maximum 45° from either axis (Silver and Chan, 1988; Bowman and Ando, 1987; Kosarev et al., 1984).

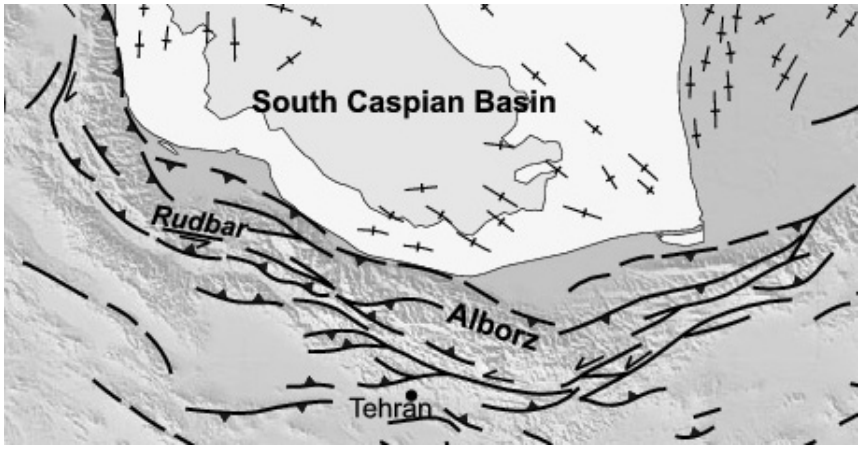

Figure 1. Tectonic map of central Alborz, (Jackson et al., 2002).

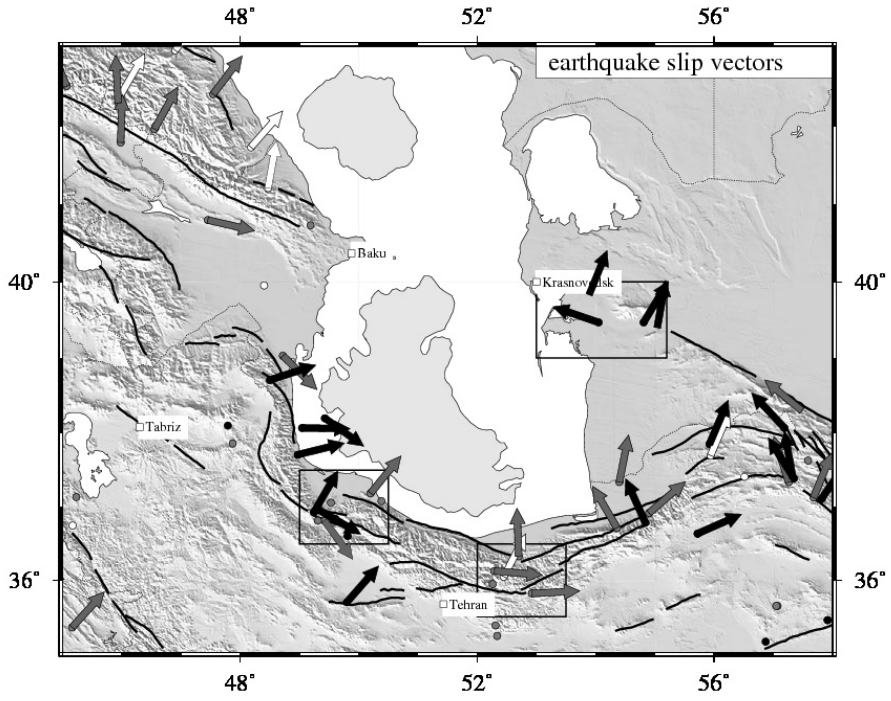

Figure 2. Horizontal projections of slip vectors of shallow earthquakes round the South Caspian Basin. ● Black arrows for events where the mechanisms are constrained by body wave modeling ● Grey arrows are for Harvard CMT events ● White arrows are for first-motion solutions. Arrows are plotted to show the motion of the south or west side relative to the north or east (Jackson et al., 2002).

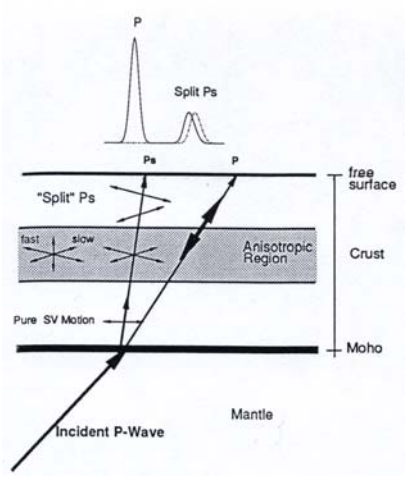

Figure 3. The effect of shear wave splitting in the Moho P to S converted phase. Top shows a schematic seismogram in the fast/slow coordinate system with split horizontal P_s components.

Beyond the preliminary analysis of P_s phase amplitude and polarity, there are three methods for analyzing splitting in the P_s phase. These methods are as follows: Particle motion analyses, Waveform cross correlation and Tangential energy minimization. All methods are similar in that they attempt to estimate the orientation and degree of anisotropy. Orientation is estimated by determining the direction of the fast azimuth of anisotropy (φ), and the degree of anisotropy is estimated by measuring the time split (δt) between the fast and slow components of motion. We selected only seismograms with impulsive Ps phases and relatively high signal-to-noise ratios for analysis. Since particle motion is a good diagnostic of shear wave splitting, we examined initial horizontal motion of the Ps phase. Those with initial linear motion and an impulsive radial P_s were assumed to be arriving along an axis of anisotropy (Silver and Chan, 1988, 1991; Kosarev et al., 1984).

4 DATA PROCESSING AND TELESEISMIC RECEIVER FUNCTION ANISTROPY IN THE ALBORZ REGION

To utilize teleseismic P waveforms, we must isolate the response of the crust and upper mantle structure beneath the station. The receiver function, is also free from the source and mantle path effects, This step is done by using source deconvolution (for a review, see Langston (1979); Ammon (1991); and Owens et al., (1984). In this study, we selected 8 events recorded at three seismic broadband stations (CHTH, DAMV and THKV) of International Institute of Earthquake Engineering and Seismology (IIEES). The information about earthquakes is shown in table 1. The 3-component seismogram of earthquake 05 September 2004 recorded at DAMV is shown in figure 4a. The receiver function obtained from this event (05 September 2004) at DAMV is shown in figure 4b. To prepare receiver function, we selected a time window of 120 seconds (30 s pre-event, 90 s post-event), doing a band pass filter of 0.05-0.7 Hz and applying a Hanning taper of 0.2, horizontal seismograms are rotated to radial and tangential components considering the theoretical backazimuth of the event. Finally the vertical component is deconvolved from the radial and tangential components in the frequency domain with water level stabilization method (Langston, 1979; Ammon, 1991). The resulting horizontal receiver functions are primarily sensitive to the shear velocity structure beneath the station (Owens et al., 1984). A strong secondary phase, on the radial component, has been observed and interpreted to be the P_s conversion from the crust-mantle boundary. The Moho P_s phase converts from a P-to-S wave nearly directly beneath the receiving station (DAMV). Thus the P_s phase from the Moho can be unambiguously picked for further study.

In the next step, we used the automated S-wave splitting technique developed by Teanby et al. (2004) to analyse the data. Most shear-wave splitting programs involve manually picking the analysis window. This creates some uncertainty as the measurement may change over different windows. Teanby et al. (2004) developed an algorithm that performs splitting analysis on a range of window lengths and positions, and then picks the window with the most stable measurement, which reduces the uncertainty in the measurement. Cluster analysis is used to find the most stable measurement.

In this study each receiver function is run through the automated shear-wave splitting program. First the shear wave arrival (P_s) is picked (the line marked S in figure 5a). Then a window is defined around the shear wave (between lines A and F in figure 5a). Then we apply the Silver and Chan (1991) method of determining splitting measurements. Particle motion will be elliptical if anisotropy is present (figure 5b, left). A grid search is performed over the fast-direction and delay time. Both components are rotated under the fast direction and one component is lagged by the delay time.

Table 1. Information of Teleseismic Events which are used for this study.

Date	Time	Lat. deg.	Long. deg.	Depth km.	Magnitude	Ref.	Dis. From DAMV(km.)
2004 09 05	100707.82	33.07	136.62	14	7.2	MwHRV	7528
2004 09 05	145718.61	33.18	137.07	10	7.4	MwGS	7558
2004 11 11	212641.15	-8.15	124.87	10	7.5	MwHRV	9006
2005 11 14	213851.42	38.11	144.90	11	7.0	MwHRV	7903
2005 12 03	161042.40	29.34	130.26	47	6.0	mb GS	7191
2005 12 09	233023.93	-6.18	29.71	10	5.5	mb GS	5172
2005 12 21	070905.17	-0.07	124.67	25	6.3	mb GS	8447
2006 01 15	115827.43	-7.82	122.59	250	6.1	mb GS	8787

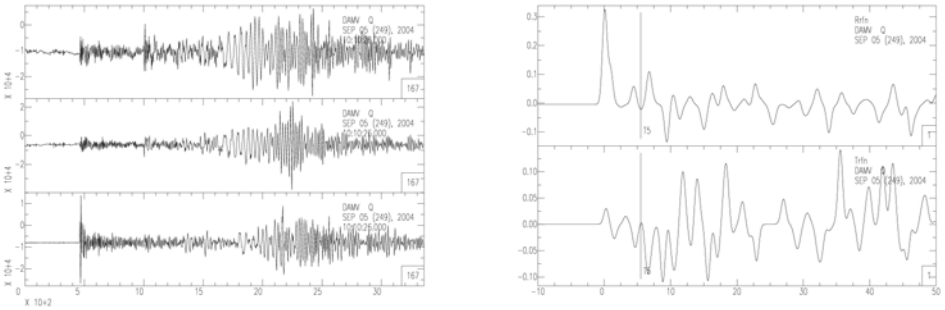

(a) **(b)**

Figure 4. (a) Three-components seismogram of the earthquake of 05 September 2004 (Mw=7.2) that were recorded at station DAMV (IIEES) in BAZ = 64.6 $^{\circ}$. (b) The corresponding radial and tangential receiver functions.

The eigenvalues of the corrected covariance matrix of particle motion are a measure of the linearity. The program looks for the φ and δt pair that has the smallest second eigenvalue and therefore the most singular corrected covariance matrix. Then an F-test is performed to calculate the 95% confidence interval, as described by Silver and Chan (1991) (see figure 5c). These steps are repeated for more windows. Any number of windows can be chosen, but the running time of the program strongly depends on the number of windows. The bounds of the windows are defined either manually by picking the maximum and minimum window size, or automatically by stating the size of the increments at the start and end of the window.

In this study 210 windows are used, varying the start of the window by 3 increments and the end of the window by 70 increments. The program then returns a measurement for each window, which is displayed in diagnostic plots (figure 6). Cluster analysis is then used to determine the optimum result, which is defined to be the lowest error in the cluster with the lowest variance. The program produces a series of diagnostic plots (figure 5 and figure 6) that are used to evaluate the stability of the result. The measurement is considered reliable if it fits the following criteria, which are based on visual checks of the plots:

1. The energy on the transverse component to the incoming polarization direction that has been corrected for splitting is minimized (figure 5a, down).
2. The fast and slow waveforms are similar and correlated after correcting for splitting (figure 5b, up).
3. Particle-motion is elliptical before and linear after the correction (figure 5b, down).
4. The error surface has a unique and well-defined solution (figure 5c), as unstable events often exhibit multiple highs.
5. The “window plot” exhibits a plateau containing many points of low error; one point on the plateau should be the solution (figure 6).

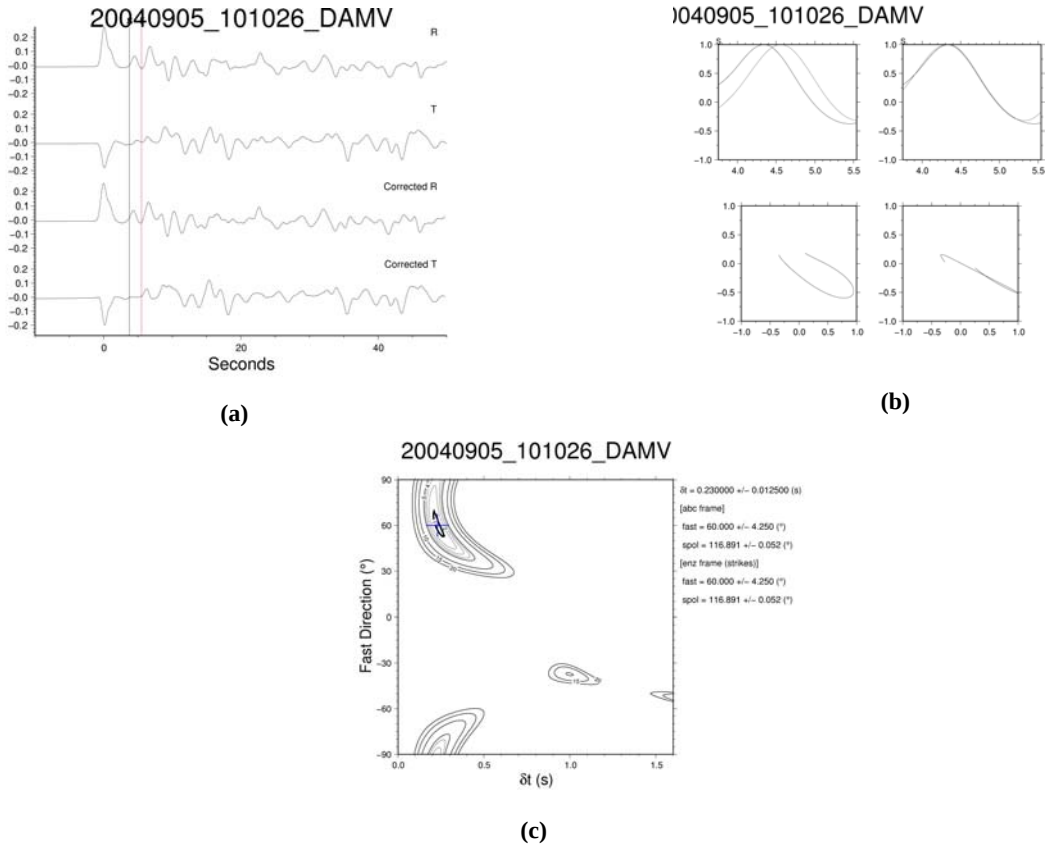

Figure 5. Diagnostic plots of a single shear-wave splitting measurement, (a) Original radial and transverse components are rotated into radial and transverse components and corrected for splitting. (b) The fast and slow component of the shear-wave before and after splitting is shown along with the associated particle motion. (c) The error surface, which is contoured according to confidence regions is the outline of the 95% confidence region.

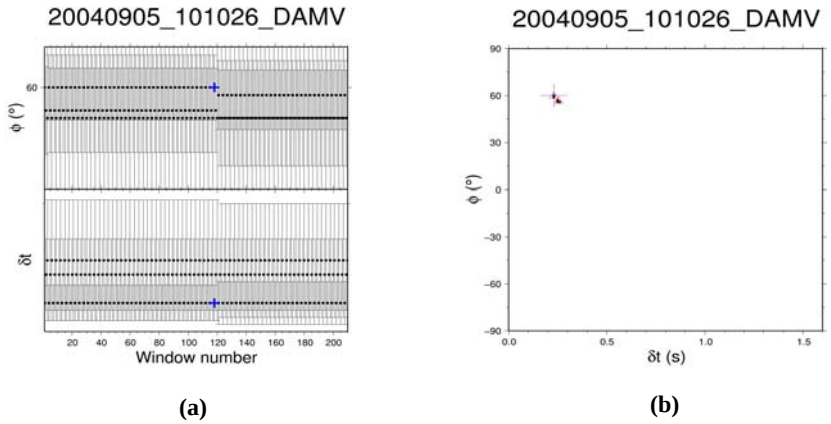

Figure 6. Diagnostic plots from the cluster analysis, on the left are the results from all windows on which shear-wave splitting analysis was performed. On the right are the clusters (triangles) and solutions from each window. The best solution is indicated by a cross in both plots.

The same processing is also performed for other two stations (DAMV, THKV and CHTH). The average values of anisotropy in the crust obtained from our processing are about (DAMV, $\varphi = 72^\circ$ and δt =0.23 sec.), (CHTH, $\varphi = 68^\circ$ and δt =0.28 sec.) and (THKV, $\varphi = 50^\circ$ and δt =0.21 sec.) beneath 3 stations.

5 DISCUSSION

It is often assumed that anisotropy in the crust, particularly at shallow depths, is a result of the preferred alignment of vertically parallel microcracks (Crampin, 1984a, b; Crampin et al., 1984a, b). Microcracks in dilatant rock are aligned with their normal parallel to the minimum principle stress. Crampin (1984a) showed that the polarization direction of fast traveling shear waves will be parallel to the plane of the crack and perpendicular to the tensile stress direction. This idea is further supported by synthetic seismogram modeling of refraction data from the 1983 Ngendei seismic refraction experiment (Shearer and Orcutt, 1986). They found seismic anisotropy in the south Pacific within the top kilometer of oceanic crust and in the uppermost mantle. Crustal anisotropy was modeled as vertical cracks oriented parallel to the fast direction. This implies that the obtained fast direction is perpendicular to the fossil spreading direction in the region, if we had spreading in the past. Conversely, the upper mantle fast direction is parallel to fossil spreading and thus is consistent with aligned olivine crystal models of anisotropy.

The NE-SW trending fast azimuth calculated from our study is roughly perpendicular to the dominant fracture systems in the Alborz region. Our results are also in good agreement with the results of Jackson et al. (2002) (figure 2).

An upper mantle source can be immediately ruled out since the P_s phase is generated at the Moho, and thus any splitting must be due to an anisotropic region between the Moho and the surface. Most of our receiver functions showed two different P_s phases on radial component. We believed that the first Ps phase is generated in the upper crust and the second belongs to the Moho border. The value of anisotropy parameter, which is given in this article, is for second P_s phases. Thus it seems reasonable to infer that the observed fast azimuth orientation is due to an anisotropic source approximately between a depth of about 15 and 30 km (the lower crust).

We use Moho P_s phases from teleseismic receiver functions to identify and estimate the shear wave anisotropy in the crust of the Alborz region. The previous section indicates that the orientation and amount of splitting we observe are consistent with reasonable petrologic models of the lower crust in the Alborz region (private commutation with Dr. A. Saeedi). The use of Moho P_s phases to study anisotropy is potentially valuable since it is one of the few ways to isolate the lower crust in the study of anisotropy. This is the first identification of shear wave anisotropy in term of crustal converted phases as far as we know. Thus some comments on the potential applicability of this technique are in order.

6 CONCLUSION

To study the anisotropy situation of the south-central Alborz region, we selected eight teleseismic earthquakes which were recorded at three seismic broadband stations (IIEES). Analysis of shear wave splitting of the Ps conversion from the crust-mantle boundary indicates a fast azimuth of anisotropy oriented approximately NE-SW. This strongly suggests coherent crustal anisotropy with a fast direction perpendicular to the strike of mountain block ranges.

We estimate the average directions of anisotropy under three stations, DAMV, THKV and CHTH of 42, 55, 55 degree, respectively. Moreover our results show that the magnitude of anisotropy are are 0.23, 0.22, 0.27 seconds, respectively, which are in good agreement with the geology and tectonic setting of the Alborz mountains.

ACKNOWLEDGEMENT

Authors are grateful to the International Institute of Earthquake Engineering and Seismology (IIEES) for preparing the necessary broadband waveforms.

REFERENCE

Ague, J. J., 1995, Deep crustal growth of Quartz, kyanite and garnet into large aperture, fluid-filled fractures, northeastern Connecticut, USA, J. Metamorph. Geol., **13**, 299-314.

Allen M. B., Ghassemi, M. R., Sharabi, M., and Qorashi, M., 2003, Accommodation of late Cenozoic oblique shortening in the Alborz range, Iran, J. Struct. Geol., **25**, 659-672.

Ammon, C. J., 1991, The isolation of receiver effects from teleseismic P waveforms. B. Seismol. Soc. Am., **81**, 2504-2510.

Asudeh, I., 1982, Seismic structure of Iran from surface and body wave data. Geophys. J. Roy. Astron. Soc., **71**, 715-730.

Babuska, V., and Cara, M., 1991, Seismic Anisotropy in the Earth (Kluwer Academic, Dordrecht.

Babuska, V., and Pros, Z., 1984, Velocity anisotropy in granodiorite and quartzite due to the distribution of microcracks, Geophys. J. Roy. Astron. Soc., **76**, 121-127.

Backus, G. E., 1962, Long-wave elastic anisotropy produced by horizontal layering, J. Geophys. Res., **67**, 4427-4440.

Bowman, J. R., and Ando, M., 1987, Shear-wave splining in the upper-mantle wedge above the Tonga subduction zone, Ceophys. J. Roy. Astron. Soc., **88**, 25-41.

Burdick, L. J., and Langston, C. A., 1977, Modeling crustal structure through the use of converted phases in teleseismic body waveforms, B. Seismol. Soc. Am., **67**, 677-691.

Chen, C. Y., Chen, W. P., and Molnar, P., 1980, The uppermost mantle P wave velocities beneath Turkey and Iran. Geophys. Res. Lett., **7**, 77-80.

Crampin, S., 1984a, An introduction to wave propagation in anisotropic media, ceophys. J. Roy. Astron. Soc., **76**, 17-28.

Crampin, S., 1984b, Effective anisotropic elastic constants for wave propagation through cracked solids, Ceophys. J. Roy. Astron. Soc., **76**, 135-145.

Crampin, S., 1991, Effects of point singularities on shear-wave propagation in sedimentary basins, Geophys. J. Int. **107**, 531-543.

Crampin, S., Chesnokov, E. M., and Hipkin, R. G., 1984a, Seismic anisotropy-The state of the art; II, Ceophys. J. Roy. Astron. Soc., **76**, 1-16.

Crampin, S., Evans, R., and Atkinson, B. K., 1984b, Earthquake prediction: A new physical basis, Ceophys. J. Roy. Astron. Soc., **76**, 147-156.

Dehghani, G. A., and Makris, J., 1984, The gravity field and crustal structure of Iran. Neues Jahrb. Geol. Palaeontol., **168**, 215-229.

De Martini, P. M., Hessami, K., Pantosti, D., D'Addezio, G., Alinaghi, H., and Gafory-ashtiani, H., 1998, A geological contribution to the evaluation of the seismic potential of the Kahrizak fault (Tehran, Iran). Tectonophysics. **287**, 187-199.

DeMets, C., Gordon, R. G., Argus, D. F., and Stein, S., 1990, Current plate motions, Geophys. J. Int., **101**, 425-478.

Doloei, J., and Roberts, R., 2003, Crust and uppermost mantle structure of Tehran region from analysis of teleseismic P-waveform receiver functions, Tectonophysics. **364**, 115-133.

Fouch, M. J., Fischer, K. M., Parmentier, E. M., Wysession, M. E., and Clarke, T. J., 2000, Shear wave splitting, continental keels, and patterns of mantle flow. J. Geophys. Res., **105(B3)**, 6255-6275.

Fouch, M. J., and Rondenay, S., 2005, Continental Seismic Anisotropy, Submitted to Phys. Earth Planet Int August 2005.

Hearn, T. M., 1996, Anisotropic Pn tomography in the western United States, J. Geophys. Res., **101**, 8403-8414.

Hudson, J. A., 1981, Wave speeds and attenuation of elastic waves in material containing cracks, Geophys. J. Roy. Astron. Soc., **64**, 133-150.

Jackson J. A., and McKenzie, D. P., 1984, Active tectonics of the Alpine-Himalayan Belt between western Turkey and Pakistan, Geophys. J. Roy. Astron. Soc., **77**, 185-246.

Jackson J., Priestley, K., Allen, M., and Berberian, M., 2002, Active tectonics of the South Caspian Basin, Geophys. J. Int., **148**, 214-245.

Kosarev, G. L., Makeyeva, L. I., and Vinnik, L. P., 1984, Anisotropy of the mantle inferred from observations of P to S converted waves, Ceophys. J. Roy. Astron. Soc., **76**, 209-220.

Langston, C. A., 1977, The effect of planar dipping structure on source and receiver responses for constant ray parameter, B. Seismol. Soc. Am., **67**, 1029-1050.

Langston, C. A., 1979, Structure under Mount Rainier, Washington, inferred from teleseismic body waves, J. Ceophys. Res., **84**, 4749-4762.

Levin, V., Menke, V., and Park, J., 1999, Shear wave splitting in the Appalachians and the Urals: A case for multilayered anisotropy, J. Geophys. Res., 104(B8): **17**, 975-993.

Lynn, H. B., 1991, Field measurements of azimuthal anisotropy: first 60 meters, San Francisco Bay Area, CA, and estimation of the horizontal stress ratio from VS1/ VS2, Geophysics. **56**, 822-832.

Mangino S. and K. Priestley (1998), The crustal structure of the southern Caspian region, Geophys. J. Int., **133**, 630-648.

McQuarrie N., Stock, J. M., Verdel, V., and Wernicke, B. P., 2003, Cenozoic evolution of Neotethys and implications for the causes of

plate motions, Geophys. Res. Lett. 30 (doi:10.1029/2003GL017992).

Owens, T. J., 1987, Crustal structure of the Adirondack mountains determined from broadband teleseismic waveform modeling, J. Ceophys. Res., **92**, 6391-6401.

Owens, T. J., Zandt, G., and Taylor, S. R., 1984, Seismic evidence for an ancient rift beneath the Cumberland Plateau, Tennessee: A detailed analysis of broadband teleseismic P waveforms, J. Ceophys. Res., **89**, 7783-7795.

Park, J., and Levin, V., 2002, Seismic anisotropy: Tracing plate dynamics in the mantle. Science, **296**(5567), 485-489.

Phinney, R. A., 1964, Structure of the Earth's crust from spectral behavior of long-period body waves, J. Ceophys. Res., **69**, 2997-3017.

Raitt, R. W., Shor Jr., G. G., Francis, T. J. G., and Morris, G. B. 1969, Anisotropy of the Pacific Upper Mantle, J. Geophys. Res., **74**, 3095-3109.

Ribe, N., 1992, On the Relation Between Seismic Anisotropy and Finite Strain, J. Geophys. Res., **97**, 8737-8747.

Savage, M. K., Silver, P. G., and Meyer, R. P., 1990, Observations of teleseismic shear-wave splitting in the Basin and Range from portable and permanent stations, Geophys. Res. Lett., **17**(1), 21-24.

Shearer, P. M., and Orcutt, J. A., 1986, Compressional and shear wave anisotropy in the oceanic lithosphere-The Ngendei seismic refraction experiment. Geophys. J. Roy. Astron. Soc., **87**, 967-1003.

Silver, P. G., 1996, Seismic anisotropy beneath the continents: probing the depths of Geology, Ann. Rev. Earth Planet. Sci., **24**, 385-432.

Si1ver, P. G., and Chan, W. W., 1988, Implications for continental structure and evolution from seismic anisotropy, Nature, **335**, 34-39.

Silver, P.G., and Chan, W. W., 1991, Shear wave splitting and subcontinental mantle deformation, J. Geophys. Res., 96(B10): **16**, 429-454.

Sobouti, F., and Arkani-Hamed, J., 1996, Numerical modelling of the deformation of the Iranian plateau. Geophys. J. Int. **126**, 805-818.

Sodoudi, F., Kind, R., Kamalian, N., and Sadidkhoy, A., 2004, The crust and upper mantle structure of the central Alborz (Iran) using teleseismic receiver function, EGU meeting 2004, Nice, France.

Teanby, N. A., Kendall, J-M., and van der Baan, M., 2004, Automation of shear wave splitting measurements using cluster analysis, B. Seismol. Soc. Am., **94**, 453-463.

Vernant Ph., Nilforoushan, F., Che´ry, F., Bayer, R., Djamour, Y., Masson, F., Nankali, H., Ritz, J. F., Sedighi, M., and Tavakoli, F., 2004, Deciphering oblique shortening of central Alborz in Iran using geodetic data, Earth Planet. Sci. Lett. **223**, 177-185.

Vinnik, L. P., Farra, V., and Romanowicz, B., 1989, Azimuthal anisotropy in the Earth from observations of SKS at GEOSCOPE and NARS broadband stations, B. Seismol. Soc. Am., **79(5)**, 1542-1558.

Vinnik, L. P., Makeyeva, L. I., Milev, A., and Usenko, A. Y., 1992, Global patterns of azimuthal anisotropy and deformations in the continental mantle, Geophys. J. Int. **111**, 433-447.

Zhang, S. and Karato, S., 1995, Lattice Preferred Orientation of olivine aggregates deformed in simple shear, Nature. **375**, 774-777.

Zhi, Z., and Schwartz, S. Y., 1994, Seismic anisotropy in the shallow crust of the Loma Prieta Segment of the San Andreas fault system, J. Geophys, Res., **99**, 9651-9661.